



SAKARYA ÜNİVERSİTESİ

# FEN BİLİMLERİ ENSTİTÜSÜ DERGİSİ

Sakarya University Journal of Science  
SAUJS

ISSN 1301-4048 e-ISSN 2147-835X Period Bimonthly Founded 1997 Publisher Sakarya University  
<http://www.saujs.sakarya.edu.tr/>

Title: A Phased Array Antenna System of a Millimeter-wave FMCW Radar for Blind Spot  
Detection of Mobile Robots

Authors: Hüseyin Şerif SAVCI

Received: 2022-06-15 00:00:00

Accepted: 2022-10-20 00:00:00

Article Type: Research Article

Volume: 26

Issue: 6

Month: December

Year: 2022

Pages: 1253-1261

How to cite

Hüseyin Şerif SAVCI; (2022), A Phased Array Antenna System of a Millimeter-wave  
FMCW Radar for Blind Spot Detection of Mobile Robots. Sakarya University Journal  
of Science, 26(6), 1253-1261, DOI: 10.16984/saufenbilder.1131504

Access link

<https://dergipark.org.tr/en/pub/saufenbilder/issue/74051/1131504>

New submission to SAUJS

<http://dergipark.gov.tr/journal/1115/submission/start>

## A Phased Array Antenna System of a Millimeter-wave FMCW Radar for Blind Spot Detection of Mobile Robots

Hüseyin Şerif SAVCI\*<sup>1</sup> 

### Abstract

Mobile robots have been extensively used in manufacturing plants for inter-logistic transportation in recent years. This paper covers a phased array antenna design for a millimeter wave radar system to improve lidar-based navigation systems' safety and environmental consciousness. The K-band phased array antenna, when integrated with 24 GHz Frequency-Modulated-Continuous-Wave (FMCW) radar, not only enhances the accuracy of the 2-D Area Scanning lidar system but also helps with the safe operation of the vehicle. The safety improvement is made by covering blind spots to mitigate collision risks during the rotations. The paper first reviews the system-level details of the 2D lidar sensor and shows the blind spots when integrated into a Mobile Robot prototype. Then continues with the inclusion of an FMCW Low-Speed Ramp radar system and discusses the design details of the proposed K-band antenna array, which will be integrated with a radar sensor.

**Keywords:** Mobile robots, lidar, FMCW radar, blind-spot detection, natural navigation, planar antenna array

### 1. INTRODUCTION

With the advancement of sensory devices, autonomous aerial, water, and ground vehicles are found in many usages, from surveillance to transportation. Autonomous Mobile Robots (MoRo) are becoming an essential part of heavy industry production plants to improve safety and reduce the risk of material and human loss and damage. Mobile Robots have been performing indoor transportation tasks in many plants without an operator. They transfer inter-

logistic production parts in factories, carry luggage in airports, and offer hotel room service. The system specs, physical constraints, and shapes may vary considerably depending

on the use case. However, they all used similar sensors and had to tackle similar problems [1].

The emergence of Industry 4.0 and intelligent plants put autonomous vehicles on the front lines of manufacturing operations to reduce the risk of operator failure and equipment loss and

\* Corresponding author: [hsavci@medipol.edu.tr](mailto:hsavci@medipol.edu.tr)

<sup>1</sup> İstanbul Medipol University, Department of Electrical and Electronics Engineering

ORCID: <https://orcid.org/0000-0002-5881-1557>



to increase overall efficiency and throughput. As the product variety has increased in the factories, more parts must be moved to the edge of the production line with highly accurate timing. Such a time-sensitive operation requires complex logistic management in an extremely dynamic environment. That is the main reason behind deploying mobile robots with self-navigating capability. For example, in a typical modern automotive assembly line, roughly 25 manual forklifts work around the clock with 80 operators [2]. However, the same assembly line can function with only eight autonomous mobile robots, resulting in the same productivity and increased safety. These numbers show that a mobile robot can amortize itself in 1.5 years. For these reasons, autonomous mobile robots will be one of the significant inter-logistic equipment in heavy-duty assembly lines of factories very soon [3].

There are several different navigation and guidance systems for mobile vehicles. The natural navigation system is the most suitable for manufacturing plants with dynamically changing environments due to its manageable implementations and fast adaptations. Also, facilities with highly hazardous environments, such as nuclear fusion reactors, benefit from autonomous mobile vehicles with navigation technologies [4]. Other systems require structural changes in plants, such as installing RF beacons and magnetic stripes as guiding tracks on the floor. These are more expensive and less flexible than natural navigation systems [5, 6].

MoRos, with natural navigation guidance systems, employ a laser-based scanning technology called Laser Detection and Ranging (lidar) [7]. These scanners are placed on the body of the vehicle. The MoRo continuously uses the lidar sensor in map generation, navigation, and environment detection for safe operation. In natural navigation systems, reference images of the vehicle's operating area are stored in the vehicle's memory. Navigation

uses data reflected from the objects around the vehicle, such as walls, columns, machines, and barriers. Positioning is found by comparing the incoming point clouds with the ones stored in the memory [8].

For the autonomous navigation of mobile robots, various sensor technologies such as ultrasonic sensors, magnetic tapes, low energy Bluetooth, UHF RFID, mono/stereo cameras, lidar, and radar-based systems are being used [9, 10]. As part of safe navigation, the precision of obstacle detection and avoidance would determine the level of safety for mobile robots. Several obstacle detection and avoidance techniques use different sensors, such as ultrasound-based, camera-based, radar-based, and lidar-based. These sensors are not only used for natural navigation and the primary localization system but also a safety alarm by constantly surveilling the surrounding against safety hazard issues [8, 11]. Each sensor has its unique strength and weakness. The camera-based systems do real-time image-capturing of the environment and perform image processing techniques on the live images [8]. In addition, several studies, such as deep learning-based intelligent surveillance, utilize only cameras [12]. However, this solution requires extensive processing power and raises some privacy concerns. For example, radar sensors lack the ability of object classification and the level of accuracy compared to other systems. Lidar is the leading technology for mobile vehicle navigation and obstacle avoidance systems. Although the costs are too high for consumer use, the lidar is still superior to the alternatives from an accuracy and safety point of view [13].

Moreover, with the lidar wavelengths around 700nm-1500nm, the system sensitivity is in the order of centimeters which meets the safety demands of inter-logistic transportation in manufacturing plants. However, lidar is not the ultimate standalone solution. The high cost of lidar units limits the number of such sensors installed on a vehicle. This limitation results in

significant safety flaws, such as blind spots. Therefore, other technologies, such as radar and camera sensors, are also being considered to complete autonomous operations [8, 11, 13, 14]. However, in the current commercial developments, neither of these sensors (lidar, radar, camera) can alone be used in mobile robots. However, each may have some advantages over others in some specific cases.

Figure 1 shows a performance comparison among three major sensor types: radar, lidar, and camera. The plot evaluates them on nine different conditions. Here 0 is the worst, and ten is the best in the corresponding category. We can see that some have superior performance for different conditions while inferior for others. None is sufficient in all situations and cases, especially detecting obstacles and blind spots. However, combining different technologies reduces the risk of failure to sufficiently cover all possible scenarios. However, the optimum combination is solely dependent on the use case. As complementary to lidar-based systems, radar comes as one of the best solutions for its high-speed operation, safe usage, privacy concerns, ruggedness against environmental factors such as smoke, dust, and dirt, and less demand for processing power. It is seen from Figure 1 that the limited horizontal resolution of the lidar would risk the mobile robot's safe operation. This limitation is addressed by integrating a radar sensor into a mobile robot's lidar-based sensing system. Finally, they together can satisfy a 360° continuous environment detection for mobile robots [8, 11].

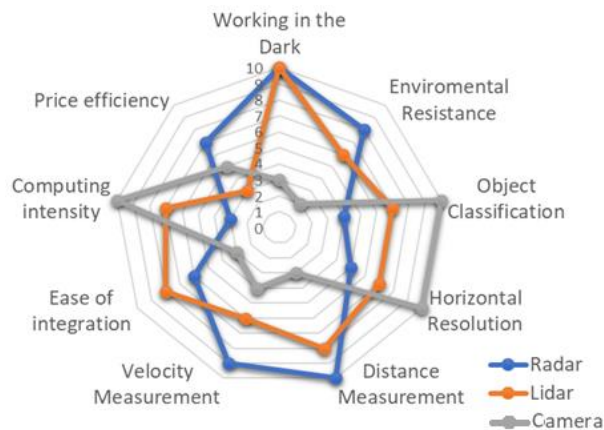


Figure 1 The capability of different sensors

## 2. SYSTEM CONSIDERATIONS

Figure 2 shows a 3D system sketch of an autonomous mobile robot. The system's power train consists of an industrial PLC, a safety PLC, two front and rear caster wheels, two DC-motor-powered driver wheels in the middle, and two lidars in the front and rear.

This study is carried out in two phases. First, in the prototype, the mobile robot prototype includes only a lidar sensor. The lidar data are obtained in a natural working environment.

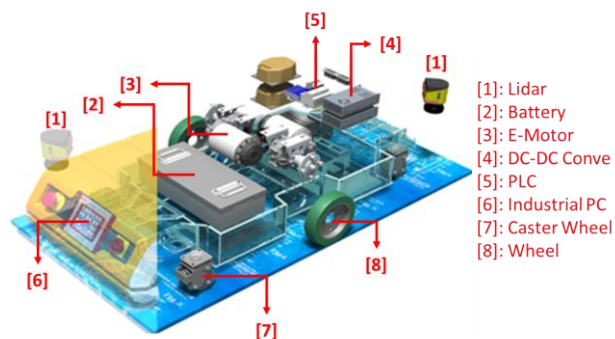


Figure 2 System Blocks of Mobile Robots

The shortcomings of lidar-only detection are found. In the second phase, commercially available millimeter wave ISM (Industrial, Scientific, and Medical) radar systems are investigated to be used as a complementary system to lidar-only detection. Analog Devices

Eval-Radar-MMIC2 24GHz FMCW, radar development kit, is selected. This radar measures the range, velocity, and angle of arrival of the objects in its range. The equipment needs a phased array antenna system. The design and measurement of the antenna system are explained in detail.

## 2.1. Lidar, Point Clouds, and Blind Spots

A lidar system detects the objects in front and behind the mobile vehicles as point clouds which are the positive pixels detected as bouncing-back laser beams from a nearby object. The 2D lidar system continuously scans the laser beam in azimuth angles and generates such time and space-variant point clouds.

Figure 3 shows the measurement data taken by the actual lidar system mounted in the front and rear bumper of a Mobile Robot. In this picture, the orange square represents the vehicle itself. The red arrow points to the direction of movement and the front side of the vehicle. Blue dots in the point cloud indicates objects around. The point cloud distributions change as time and vehicle progress. Data shown here is from the same instance of time and state of the vehicle. A dynamic map is generated by combining the front and rear lidar raw data when data is processed on the static map. It is seen from this figure that lidar helps the navigation of the vehicle by constantly detecting the objects around it. Each lidar scans an area with an angle of  $210^\circ$ . However, it is also seen that there are regions marked with yellow question marks that are unreachable by any of the lidar laser beams. Each of these regions corresponds to an angle of roughly 30 degrees midway on both sides of the vehicle. These unlit regions are called blind spots, which cause significant safety risks. Therefore, it is crucial to detect any static or moving object in these areas to be able to make a sudden left or right turn safely.

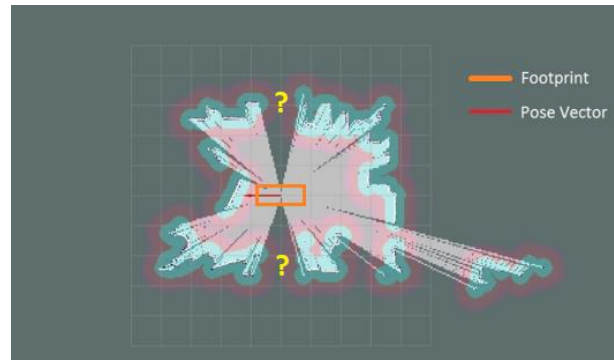


Figure 3 lidar beams coverage and blind spots

The lidar technology's cost and size limit the number of sensors to be used in a mobile robot. Thus, a radar sensor is adopted to improve the coverage and detection of objects in the blind spot, which ultimately increases the vehicle's safety and enhances the accuracy of navigation maps.

## 2.2. Radar and Antenna Arrays

Radar technology only found its usage in the aviation and defense industry (ADEF) for many decades due to its high cost and bulky size up until the 2000s. Over the last two decades, integrating RF and digital parts of entire transceiver circuits in Silicon-based semiconductor technologies such as SOI-CMOS and SiGe BiCMOS enabled its wide usage in many commercial applications and reduced overall cost tremendously [15]. In recent years, radar is becoming a standard part of Advanced Driver Assistance Systems (ADAS) in many automobiles. Including radar for blind spot detection, short-range and long-range collision avoidance, parking assistance, lane tracking/changing assistance, vital function monitor, gesture recognition, and contactless infotainment has dramatically improved the safety, security, and comfort of the vehicles.

A Frequency Modulated Continuous Wave (FMCW) radar can obtain various information concerning the detected objects using a chirp signal with a linearly increasing frequency over

a specific period. The received signal bounced from an object is mixed with a signal the same as the transmitted one, generating a down-converted intermediate frequency signal, IF. The information related to the object is determined by analyzing this IF signal. Like the wavelength of the lidar laser beams, the frequency, and bandwidth of the transmitted radar signal limit detection resolution. The more the time duration of linear-frequency-increasing chirp (namely, the larger its bandwidth), the finer the resolution for the detection of radar. So, the range resolution depends on the bandwidth swept by the chirp. However, since Analog-to Digital Converter would digitize the IF signal, its sampling rate also limits the radar's maximum range. Thus, the larger the chirp bandwidth, the better the range resolution. Also, the larger the IF bandwidth, the faster the chirps, and the better the maximum distance.

The radar makes it possible to detect the moving object's distance, arrival time, movement direction, and speed. There are two different architectures for radar systems used in the current automotive applications: the Frequency-Modulated Continuous Wave (FMCW) radar and the Pulse-Doppler radar. FMCW is used in %90 of the existing applications. The FMCW radar has two types related to the RF signal it sends for detection. LSR- Low-Speed Ramp and HSR- High-Speed Ramp according to the speed of the sent ramp sign. The most common one is LSR, with %60 usage in today's market. It does the detection by sending a triangle ramp sign with a rise time of 3ms. HSR, which utilizes the trapezoidal wave changing between the range of 20s and 100s for the measurements, is used in %30 of the market. Pulse-Doppler radars are used in the remaining %10 of the automotive market radar applications. It is possible to immediately measure an object's speed and distance by sending many sequential pulse trains. In this work, Analog Devices' EVAL-RADAR-MMIC2 radar kit is adopted. EVAL-RADAR-

MMIC2 is an Evaluation Board for a 24 GHz LSR FMCW-based radar system. Various frequencies were investigated for the radar system to improve the resolution. However, due to the limitation of measurement equipment and availability of the design kits 24GHz ISM band is preferred.

Figure 4 shows the block diagram of the 24GHz LSR-based FMCW radar system. The signal chain chipsets are ADF5901, a 24 GHz VCO and PGA with 2-Channel PA Output; ADF5904, a 4-Channel, 24 GHz receiver Downconverter; and ADF4159 which is a Direct Modulation/Fast Waveform Generating, 13 GHz, Fractional-N Frequency Synthesizer. They are all developed for commercial use in ADAS and industrial applications.

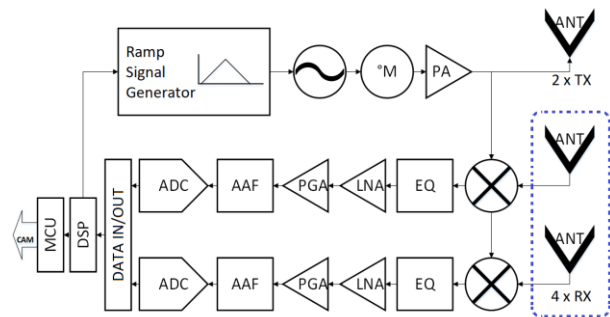


Figure 4 ISM Radar Phased Array Antennas

The system has a transmitter and receiver antenna system. The transmit antenna is like the receive antenna but only has two independent radiating elements instead of 4. The system operates in full duplex mode to support both transmit and receive. For phased array antenna, different topologies and technologies got studied. Although the end-fired antennas, such as the Vivaldi type, have superior performance in gain and directivity, their radiation pattern is perpendicular to the PCB's normal vector, which has a problematic installation on the flat body of the MoRo. Due to the production cost and ease of implementation, the microstrip patch antenna in series and the parallel combination is preferred for the arrays. Initially, a patch antenna at 24.35 GHz with

linear polarization is designed on a 6-mil Rogers substrate with a dielectric constant of 3.48. The antenna sizes (Width  $W$  and Length  $L$ ) were obtained using the following design formula [16]. The inset opening was used to allow the feed line to connect to the low-impedance point of the antenna. The length of this inset,  $x_p$ , was calculated according to equation 3. The spacing of the inset was chosen as 200 $\mu$ m, dictated by the PCB vendor as the minimum manufacturable spacing with reasonable precision.

$$W = \frac{c}{2f_m \sqrt{\epsilon_{reff}}} \quad (1)$$

$$L = \frac{c}{2f_m \sqrt{\epsilon_{reff}}} - L_{fringe} \quad (2)$$

$$x_p = \frac{\cos^{-1}\left(\sqrt{\frac{R_i}{R_e}}\right)}{\pi} L \quad (3)$$

$$\epsilon_{reff} = \frac{\epsilon_r + 1}{2} + \frac{\epsilon_r - 1}{2} \left[1 + 12 \frac{h}{W}\right]^{-1/2} \quad (4)$$

Here,  $W$  is the patch width,  $L$  is the patch length,  $c$  is the speed of light,  $h$  is substrate height,  $f_m$  is the working frequency of the antenna,  $\epsilon_{reff}$  is the effective dielectric constant,  $L_{fringe}$  is the patch length due to the fringing electric field,  $x_p$  is the inset length,  $R_i$  is the feeding line impedance, and  $R_e$  is the patch edge impedance.

The sizes of antenna design were further optimized using a Method-of-Moments-based EM simulator for an operation at 24.35GHz. The final dimensions were obtained for patch width and length as 3220 $\mu$ m x 4120 $\mu$ m. A 5.1dBi maximum gain was obtained from this patch antenna according to the simulation results.

However, higher gain performance is targeted for the system requirements. Based on the designed single patch, a 4-element parallel antenna array is developed to enhance the gain. Additionally, 4-patch antennas were placed at

$\lambda/2$  distance from each other. Each antenna was designed according to 50 $\Omega$  impedance, and  $\lambda/4$  impedance converter lines were used to adapt 25 $\Omega$  impedance, which occurs when two antennas are connected parallel, to the system impedance of 50 $\Omega$ . Each patch's theoretical extra 3dBi gain contribution is limited due to the feedline losses. Figure 5 shows the simulation results for the four-element-patch array. The antenna system has a resonance of about 24.35 GHz with 10.3dBi gain.

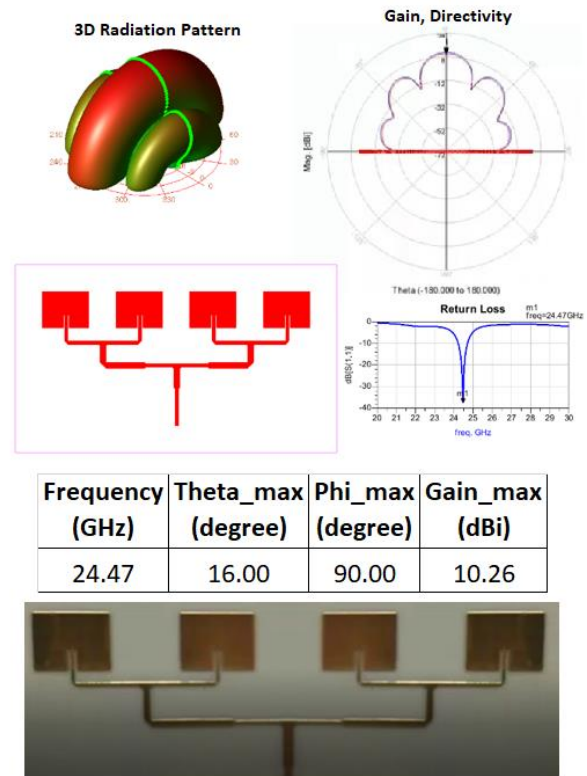


Figure 5 The antenna system with four parallel inset elements: Layout, simulated 3D radiation pattern, 2D polar pattern, return loss, gain, directivity, and tabulated summary

A 4-port 4x4 microstrip antenna array is designed to increase the antenna's gain further. The antenna is changed from an inset-fed structure to a probe-fed form using a multi-layer PCB for properly routing the feeding networks. The design is carried out using the equations in [17].

As shown 6-a, the design has 16 elements, each of which has dual-probe-fed ports and a stripline feeding network. The vertical antenna on a single column is parallel connected and fed from a single input. The design has 4 of these placed half-wavelengths. The antenna array is mounted on a Perfect Electric Conductor (a copper plate) to replicate the mobile robot body, as shown in Figure 6-b. Here port#2 is measured on the VNA while all other ports are terminated.

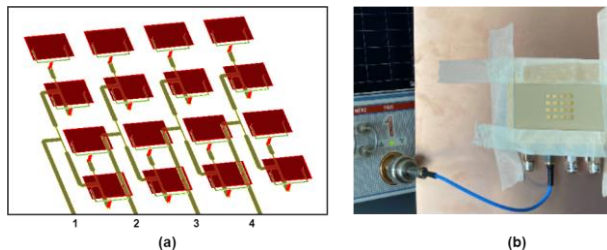


Figure 6 (a) Antenna array and feed network (b) measurement setup

Figure 7 shows the reflection coefficient in decibels, dB(S22). It is seen from the graph that the antenna system has broadband response starting from 24.45GHz and going beyond 30.65GHz with a 15dB reflection coefficient.

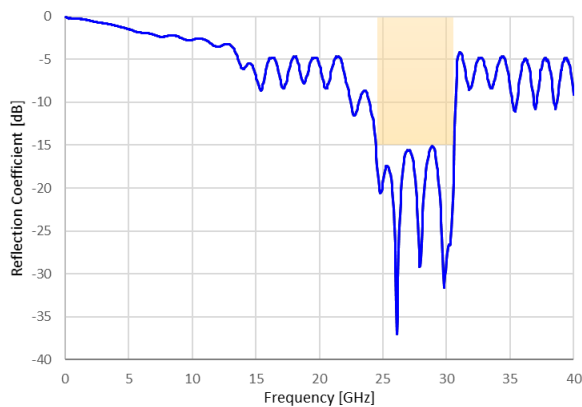


Figure 7 Single Port reflection coefficient in dB

The 2D pattern is measured using a reference antenna and RMS power detector. Figure 8 shows the antenna's radiation pattern when all ports are excited with equal phase and magnitude. The array shows a 20-degree

beamwidth and 16.2 dBi gain in its maximum direction.

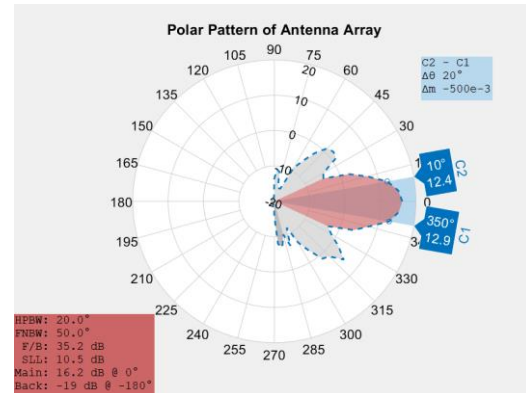


Figure 8 Radiation pattern under all ports equal-excitation

### 3. CONCLUSION

This study analyses the safety and accuracy of lidar-based navigation of industrial mobile robots. Data obtained from lidar for natural navigation reveals that due to the position of lidar sensors, there are unavoidable blind regions on the sides of vehicles that pose a high risk of collision during sudden and abrupt turns. For example, a millimeter wave ISM band FMCW automotive radar sensor with Low-Speed Ramp is used along with the proposed antenna system. The design steps, working principals, and simulated and measured results of the proposed 4-channel receiving antenna system are explained in detail. Finally, integrating lidar and radar sensors would give the mobile robots a continuous 360-degree peripheral consciousness.

#### Funding

The author has not received any financial support for this study's research, authorship, or publication.

#### The Declaration of Conflict of Interest/ Common Interest

No conflict of interest or common interest has been declared by the authors.



### ***The Declaration of Ethics Committee Approval***

This study does not require ethics committee permission or any special permission.

### ***The Declaration of Research and Publication Ethics***

The authors of the paper declare that they comply with the scientific, ethical, and quotation rules of SAUJS in all processes of the paper and that they do not make any falsification on the data collected. In addition, they declare that Sakarya University Journal of Science and its editorial board have no responsibility for any ethical violations that may be encountered, and that this study has not been evaluated in any academic publication environment other than Sakarya University Journal of Science.

### **REFERENCES**

- [1] M. Karamuk, I. H. Savci, H. Ocaklı, "A Survey on Traction System Development of Automated Guided Vehicles," *European Journal of Technique*, vol. 12, no. 1, pp. 1-12, Jun. 2022.
- [2] I. H. Savci, A. Yilmaz, S. Karaman, H. Ocaklı, H. Temeltas, "Improving Navigation Stack of a ROS-Enabled Industrial Autonomous Mobile Robot (AMR) to be Incorporated in a Large-Scale Automotive Production," *The International Journal of Advanced Manufacturing Technology*, vol. 120, pp. 3647–3668, Mar. 2022.
- [3] M. Qi, X. Li, X. Yan, C. Zhang, "On the evaluation of AGVS-based warehouse operation performance," *Simulation Modelling Practice and Theory*, vol. 87, pp. 379-394, Sep. 2018.
- [4] A. Vale, R. Ventura, R. Lopes, I. Ribeiro, "Assessment of navigation technologies for automated guided vehicle in nuclear fusion facilities," *Robotics and Autonomous Systems*, vol. 97, pp. 153-170, 2017.
- [5] G. Bocewicz, Z. Banaszak, I. Nielsen, W. Muszynski, "Re-scheduling of AGVs steady-state flow," *IFAC-Papers On-Line*, vol. 50 no. 1, pp. 3493-3498, Jul. 2017.
- [6] H. Balaji, S. Shaikh, A. Phalke S. Jadhav, "Design and methodology of automated guided vehicle - a review," *IOSR Journal of Mechanical and Civil Engineering*, vol. 1, pp. 29-35, May 2022.
- [7] S. Quan, J. Chen, "AGV Localization Based on Odometry and LiDAR," *2nd World Conference on Mechanical Engineering and Intelligent Manufacturing*, pp. 483-486, Nov. 2019.
- [8] A. Rangesh, M. M. Trivedi, "No blind spots: full-surround multi-object tracking for autonomous vehicles using cameras and lidars," *IEEE Transactions on Intelligent Vehicles*, vol. 4, no.4, pp. 588-599, Dec. 2019.
- [9] R. P. Mahapatra, S. V. Kumar, G. Khurana, R. Mahajan, "Ultrasonic sensor-based blind spot accident prevention system," *International Conference on Advanced Computer Theory and Engineering*, pp. 992-995, Dec. 2008.
- [10] S. Lee, H. Wang, "Navigation of automated guided vehicles using magnet spot guidance method," *Robotics and Computer Integrated Manufacturing*, vol. 28, no. 3, pp. 425-436, Jun. 2012.
- [11] G. Liu, L. Wang, S. Zou, "Radar-based blind spot detection and warning system for driver assistance," *IEEE 2nd Advanced Information Technology*,

Electronic and Automation Control Conference, pp. 2204-2208, Mar. 2017.

- [12] Y. Shen, W. Q. Yan, "Blind spot monitoring using deep learning," International Conference on Image and Vision Computing New Zealand, Auckland, pp. 1-5, Nov. 2018.
- [13] A. Hiçdurmaz, A. Tuncer, "Real-Time Obstacle Avoidance Based on Floor Detection for Mobile Robots," Sakarya University Journal of Science, vol. 24, no. 5, pp. 845-853, Oct. 2020.
- [14] J. Verhaever, "Detection of vulnerable road users in blind spots through Bluetooth low energy," Progress in Electromagnetics Research Symposium - Spring (PIERS), pp. 227-231, May. 2017.
- [15] D. Saunders, S. Bingham, G. Menon, D. Crockett, J. Tor, R. Mende, M. Behrens, N. Jain, A. Alexanian, Rajanish, "A single-chip 24 GHz SiGe BiCMOS transceiver for low cost FMCW airborne radars," Proceedings of the IEEE 2009 National Aerospace & Electronics Conference, pp. 244-247, Jul. 2009.
- [16] T. Milligan, Modern Antenna Design, Wiley-IEEE Press, New Jersey, 2005.
- [17] A. Elsherbeni, P. Nayari, C.J. Reddy, Antenna Analysis and Design Using FEKO Electromagnetic Simulation Software, SciTech Publishing, New Jersey, 2014.